

# Possibility of Antimagnetic Rotation in odd-A Cd isotopes

Santosh Roy\* and S. Chattopadhyay

*Saha Institute of Nuclear Physics, 1/AF Bidhannager Kolkata, 700 064, India*

(Dated: November 8, 2018)

## Abstract

The classical particle plus rotor model for antimagnetic rotation (AMR) has been used to investigate the possibility of observation of AMR in the high spin levels of  $^{105,107,109}\text{Cd}$ . The calculated  $I(\omega)$  plot and  $B(E2)$  values have been compared with the available experimental data.

**PACS numbers:** 21.10.Re, 21.10.Tg, 21.60.Ev, 23.20.-g, 27.60.+j

**Keywords:** AntiMagnetic Rotation, classical particle rotor model, odd-A Cd

arXiv:1012.1751v1 [nucl-th] 8 Dec 2010

---

\* Also at S. N. Bose National Centre for Basic Sciences. Block JD, Sector III, Saltlake City, Kolkata 700098, India

## I. INTRODUCTION

The different manifestations of Shears mechanism has been found in Cd-isotopes, namely M1 band ( $^{110}\text{Cd}$ ) [1], band crossing in M1 band ( $^{108}\text{Cd}$ ) [2] and antimagnetic rotation (AMR) ( $^{106, 108, 110}\text{Cd}$ ) [3–5]. All these observed features have been well described by the geometrical model of Shears mechanism.

Recently a systematic study of antimagnetic rotation have been carried out for the even-even Cd-isotopes, namely  $^{106, 108, 110}\text{Cd}$  within the framework of classical particle rotor model [5]. In this work, observed  $I(\omega)$  plots and the measured  $B(E2)$  values for all the three isotopes have been well reproduced by this model calculations.

The vector diagram for the particle and hole angular momenta coupling scheme for AMR is shown in Fig. 1 which corresponds to a symmetric double shear structure. For Cd isotopes, there are two proton holes in the  $g_{\frac{3}{2}}$  orbitals whose angular momenta ( $\mathbf{j}_{\pi}$ ) are along the symmetry axis, while the angular momentum of the neutron ( $\mathbf{j}_{\nu}$ ) particles in  $h_{\frac{11}{2}}/g_{\frac{7}{2}}/d_{\frac{5}{2}}$  orbitals are along the rotational axis [3, 4]. Thus,  $j_{\pi} = \frac{9}{2}$  and  $j_{\nu} = a * j_{\pi}$ , where ‘a’ is the ratio of the magnitude of proton and neutron angular momentum for a specific single particle configuration. The only important degree of freedom for this model is the angle between  $\mathbf{j}_{\pi}$  and  $\mathbf{j}_{\nu}$  and is known as the shears angle ( $\theta$ ). Due to the symmetry of the double shear, the angle between the two hole vectors is  $2\theta$ . The interactions between these particle-hole and the hole-hole blades can be modeled as  $P_2$ -type forces [6]. It has been argued by Macchiavelli et. al., that such an interaction may be mediated through the core by a particle-vibrational coupling involving quadrupole phonon [7]. The systematic study of AMR in even-even Cd-isotopes indicates that the strengths of these particle-hole and hole-hole interactions are 1.2 MeV and 0.15 – 0.2 MeV, respectively, for this mass region [5].

In the present work, a systematic theoretical study has been presented for  $^{105, 107, 109}\text{Cd}$  and the calculated  $I(\omega)$  plot and measured  $B(E2)$  values have been compared with the available experimental data.

## II. CLASSICAL PARTICLE-ROTOR MODEL FOR AMR

In this model the energy  $E(I)$  is given by [5],

$$E(I) = \frac{(\mathbf{I} - \mathbf{j}_\pi - \mathbf{j}_\nu)^2}{2\mathfrak{S}} + \frac{V_{\pi\nu}}{2} \left( \frac{3\cos^2\theta - 1}{2} \right) + \frac{V_{\pi\nu}}{2} \left( \frac{3\cos^2(-\theta) - 1}{2} \right) - \frac{V_{\pi\pi}}{n} \left( \frac{3\cos^2(2\theta) - 3}{2} \right) \quad (1)$$

where the first term is the rotational contribution and the rest of the terms are the shear contributions,  $V_{\pi\nu} = 1.2$  MeV and  $V_{\pi\pi} = 0.2$  MeV. ‘n’ is the scaling factor between  $V_{\pi\nu}$  and  $V_{\pi\pi}$  and is determined by the actual number of particle-hole pairs for a given single-particle configuration.

The corresponding total angular momentum can be evaluated by imposing the energy minimization condition as a function of  $\theta$  and is given by,

$$I = aj + 2j \cos\theta + \frac{1.5\mathfrak{S}V_{\pi\nu} \cos\theta}{j} - \frac{6\mathfrak{S}V_{\pi\pi} \cos 2\theta \cos\theta}{nj} \quad (2)$$

The first two terms represents the contribution from shears mechanism ( $I_{sh}$ ) as is evident from Fig. 1. At the band head ( $\theta = 90^\circ$ ),  $I = j_\nu = aj$ , which corresponds to the aligned angular momentum of the neutrons due to core rotation. This implies that there is a band head frequency which corresponds to the alignment frequency of the neutrons which is essential for the formation of the shear structure. The higher momentum states are formed by gradual closing of the shears angle and the maximum angular momentum ( $I_{sh}^{max}$ ) that can be generated through AMR due to complete alignment of the two proton holes ( $\theta = 0^\circ$ ) in  $g_{9/2}$  orbital is

$$I_{sh}^{max} = j_\nu + \frac{9}{2} + \frac{7}{2} \quad (3)$$

The significance of the third and fourth terms of Eq. 2 becomes apparent if we determine the expression for the frequency associated with the shears mechanism ( $\omega_{sh}$ ). This can be computed through  $\left(\frac{dE_{sh}}{d\theta}\right) / \left(\frac{dI_{sh}}{d\theta}\right)$  and is given by,

$$\omega_{sh} = (1.5V_{\pi\nu}/j) \cos\theta - (6V_{\pi\pi}/nj) \cos 2\theta \cos\theta \quad (4)$$

Thus, the third and fourth terms of the Eq. 2 are equal to the product of rotational moment of inertia  $\mathfrak{S}$  and shears frequency ( $\omega_{sh}$ ). They represent the interplay between collective and shears mechanism and Eq. 2 can be re-written as

$$I = I_{sh} + \mathfrak{S}\omega_{sh} \quad (5)$$

It is to be noted that the magnitude of  $\Im$  determines the extent of the interplay in generation of angular momentum in AMR+rotation model. This value can be estimated from Eq. 5

$$\Im\omega_{sh}|_{(\theta=0^\circ)} = I_{max} - I_{sh}^{max} \quad (6)$$

where,  $I_{max}$  is the highest observed angular momentum state,  $I_{sh}^{max}$  is given by Eq. 3 and

$$\omega_{sh}|_{\theta=0^\circ} = \left( \frac{1.5V_{\pi\nu}}{j} \right) - \left( \frac{6V_{\pi\pi}}{nj} \right) \quad (7)$$

In case of AMR+rotation model, the rotational frequency ( $\omega$ ) is given by

$$\omega = \omega_{rot} - \omega_{sh} \quad (8)$$

where  $\omega_{rot} = \frac{1}{2\Im_{rot}}(2I + 1)$  is the core rotational frequency and  $\Im_{rot}$  is the core moment of inertia, whose value can be estimated from the slope of the  $I(\omega)$  plot for the ground state band (before the neutron alignment). The relative negative sign in Eq. 7 indicates that a given angular momentum state for AMR+rotation will be formed at a lower frequency as compared to that due to pure rotation.

Thus, all the parameters of the present model can either be fixed from experimental data or from the systematics of the mass region. Using Eq. 5 and Eq. 8, the theoretical  $I(\omega)$  plots have been calculated for  $^{105,107,109}\text{Cd}$  with  $V_{\pi\nu} = 1.2$  MeV and  $V_{\pi\pi} = 0.2$  MeV.

The B(E2) values have been calculated following the expression [9]

$$B(E2) = \frac{15}{32\pi}(eQ_{eff})^2 \sin^4\theta \quad (9)$$

where  $eQ_{eff} \sim 1.1$  eb can be used for all the Cd-isotopes since they have similar deformation and value of  $eQ_{eff}$  is almost solely determined by the two proton holes [4]. It has been demonstrated in the case of  $^{110}\text{Cd}$  [5], that the B(E2) values fall slowly in case of AMR+rotation as compared to pure AMR as the shear angle closes from  $90^\circ$  to  $0^\circ$  over a larger angular momentum range.

### III. RESULTS

#### A. $^{109}\text{Cd}$

The negative parity yrast sequence of  $^{109}\text{Cd}$  [10] is shown in Fig. 2(a). The high spin levels beyond  $31/2^-$  originates due to  $(\pi g_{(9/2)}^{-2}) \otimes \nu(h_{11/2})^3$  configuration. For these levels the

measured  $\mathfrak{S}^{(2)}/B(E2)$  ratio was found to be around  $165 \hbar^2 \text{ MeV}^{-1} (eb)^{-2}$  which is an order of magnitude larger than that expected for a well deformed rotor. Thus, it was concluded that these levels originate due to AMR [10].

The AMR band head spin ( $j_\nu$ ) for this configuration is  $27/2 \hbar$  ( $11/2\hbar + 9/2\hbar + 7/2\hbar$ ) which is shifted by  $2\hbar$  due to core rotation. A similar situation has been observed in  $^{106}\text{Cd}$  [3]. The double shear structure is formed by the three aligned neutrons and the two proton holes. Thus, there are six possible particle-hole pairs and one hole-hole pair which indicates  $n = 6$  in Eq. 1. This band has been established up to  $51/2 \hbar$  ( $I_{max}$ ) while  $I_{sh}^{max} = 47/2 \hbar$ . Thus,  $\mathfrak{S}\omega_s h|_{(\theta=0^\circ)} = 2 \hbar$  which gives  $\mathfrak{S} = 6 \text{ MeV}^{-1} \hbar^2$  from Eq. 6.  $\mathfrak{S}_{rot}$  has been found to be  $15 \text{ MeV}^{-1} \hbar^2$ , which is the slope of the  $I(\omega)$  plot for the ground state band. This is shown in Fig. 3(a) by the dotted line that has been shifted by  $\sim 4\hbar$  which corresponds to the aligned angular momentum of the valance neutron of  $^{109}\text{Cd}$ .

With this set of fixed parameters, the  $I(\omega)$  plot for the neutron aligned yrast band of  $^{109}\text{Cd}$  has been calculated and shown as the solid line in Fig. 3(a). The calculated frequencies have been shifted by the band head frequency of 0.51 MeV. It is evident from the figure that the AMR configuration is non-yrast over the entire frequency range. The calculated  $B(E2)$  values are shown by the solid line in Fig 3(b). It is apparent that the measured  $B(E2)$  values are about twice as large as that predicted by the model.

Thus, the present calculations seem to indicate that the high spin yrast levels of  $^{109}\text{Cd}$  do not originate due to AMR.

## B. $^{105}\text{Cd}$

The negative parity yrast sequence of  $^{105}\text{Cd}$  [11] has been established upto  $47/2^-$  and is shown in Fig. 2(b). The levels beyond  $23/2^-$  originate due to  $\pi g_{9/2}^{-2} \otimes \nu[h_{11/2}, (g_{7/2}/d_{5/2})^2]$  configuration and the lifetimes of these levels have not been measured [11]. For this configuration  $n = 6$  and the AMR band head is  $23/2 \hbar$  [ $11/2 \hbar + 7/2 \hbar + 5/2 \hbar$ ]. This implies that  $I_{sh}^{max} = 39/2 \hbar$ . Thus, for  $^{105}\text{Cd}$ ,  $\mathfrak{S}\omega_{sh}|_{(\theta=0^\circ)} = 4 \hbar$ . This leads to  $\mathfrak{S} = 11.2 \text{ MeV}^{-1} \hbar^2$ . The value for  $\mathfrak{S}_{rot}$  has been found to be  $14 \text{ MeV}^{-1} \hbar^2$  in the same way as described for  $^{109}\text{Cd}$ .

The experimental and calculated  $I(\omega)$  plot for the neutron aligned band have been shown in Fig. 6(a), where the calculated frequencies have been shifted by the band head frequency ( $\sim 0.4 \text{ MeV}$ ). It is interesting to note that the AMR configuration is non-yrast at lower

frequencies but becomes yrast around  $\hbar\omega = 0.60$  MeV which corresponds to  $35/2 \hbar$  level. Thus, the levels beyond  $31/2 \hbar$  are expected to originate due to AMR. Fig. 6(b) shows the predicted B(E2) values over the entire frequency range. The predicted B(E2) values for  $31/2 \hbar$  ( $\theta = 73.5^\circ$ ),  $35/2 \hbar$  ( $\theta = 64.5^\circ$ ) and  $39/2 \hbar$  ( $\theta = 54^\circ$ ) levels are  $0.15$ ,  $0.12$  and  $0.07 (eb)^2$ , respectively.

The present model predicts that the levels beyond  $31/2 \hbar$  originates due to an interplay between AMR and collective rotation. This prediction can be established by measuring the B(E2) transition rates for the levels beyond  $31/2 \hbar$  and comparing them with the predicted values.

### C. $^{107}\text{Cd}$

The negative parity yrast sequence of  $^{107}\text{Cd}$  [12] is known only upto  $31/2 \hbar$  (shown in Fig. 2(c)), which needs to be extended in order to investigate the possibility of AMR in  $^{107}\text{Cd}$ . The aligned angular momenta ( $i$ ) of  $^{105,107}\text{Cd}$  has been plotted against the rotational frequency ( $\hbar\omega$ ) in Fig. 5. It is apparent from the figure that the alignment gain is similar in the two cases and is around  $4\hbar$ . Thus, the neutron aligned yrast configuration for  $^{107}\text{Cd}$  is also expected to be  $(\pi g_{9/2}^{-2}) \otimes [h_{11/2}, (g_{7/2}/d_{5/2})^2]$ , which is same as that of  $^{105}\text{Cd}$ .

Since this band has not been observed upto the highest spin, the  $I(\omega)$  plot has been calculated for three possible values of  $\mathfrak{S}\omega_{sh}|_{(\theta=0^\circ)} = 2\hbar, 4\hbar$  and  $6\hbar$  and the predicted values are shown in Fig. 6(a) with dashed, solid and dot-dashed lines, respectively, for  $\mathfrak{S}_{rot} = 14 \text{ MeV}^{-1} \hbar^2$ . Once the higher spin levels of this band is established,  $\mathfrak{S}\omega_{sh}|_{\theta=0^\circ}$  will get fixed as for this band  $I_{sh}^{max} = 39/2\hbar$ . Thus, the model calculations will have a definitive prediction of  $I(\omega)$  behavior of the band if it originates due to AMR+rotation.

The predicted B(E2) values are shown in Fig.6 (b) for  $\mathfrak{S}\omega_{sh}|_{(\theta=0^\circ)}$ . A comparison of the experimental values with these predicted values will be an additional check to establish whether the high spin levels of  $^{107}\text{Cd}$  originate due to AMR+rotation.

## IV. CONCLUSION

The classical particle rotor model has been applied for three odd-A isotopes of Cd, namely  $^{105,107,109}\text{Cd}$ , where AMR is expected since this excitation mode has been reported in their

even-even partners. A comparison of  $I(\omega)$  plot and  $B(E2)$  values for  $^{109}\text{Cd}$  seems to indicate that the high spin levels do not originate due to Shears mechanism. On the other hand, levels beyond  $31/2 \hbar$  in  $^{105}\text{Cd}$  is predicted to originate due to an interplay of antimagnetic and collective rotation. However this prediction can only be established through the measurement of  $B(E2)$  transition rates for these levels. In case of  $^{107}\text{Cd}$ , the negative parity yrast band have not been established. Thus, model dependent predictions for  $I(\omega)$  plot and  $B(E2)$  values have been presented.

These calculations complement those performed for even-even Cd isotopes within a common framework of a classical particle rotor model where  $V_{\pi\pi} = 1.2 \text{ MeV}$  and  $V_{\pi\nu} = 0.2 \text{ MeV}$  have been used for all the Cd-isotopes, namely  $^{105-110}\text{Cd}$ .

- 
- [1] R.M. Clark *et al.*, Phys. Rev. Lett. **82**, 3220 (1999).
- [2] Santosh Roy *et al.*, Phys. Rev. C **81**, 054311 (2010)
- [3] A. J. Simons *et al.*, Phys. Rev. Lett. **91**, 162501 (2003).
- [4] P. Datta *et al.*, Phys. Rev. C **71**, 041305(R) (2005).
- [5] Santosh Roy *et al.*, Physics Letters B (2010), doi:10.1016/j.physletb.2010.10.018
- [6] A.O. Macchiavelli *et al.*, Phys. Rev. C **57**, R1073 (1998).
- [7] A.O. Macchiavelli *et al.*, Phys. Rev. C **58**, R621R623 (1998).
- [8] M. Sugawara *et al.*, Phys. Rev. C **79**, 064321 (2009).
- [9] R.M. Clark and A. O. Macchiavelli, Annu. Rev. Nucl. Part. Sci. **50**, 1 (2000).
- [10] C. J. Chiara *et al.*, Phys. Rev. C **61**, 034318 (2000).
- [11] D. Jerrestam *et al.*, Nucl. Phys. **A593**, 162 (1992).
- [12] Dan Jerrestam *et al.*, Nucl. Phys. **A545**, 835 (1992).

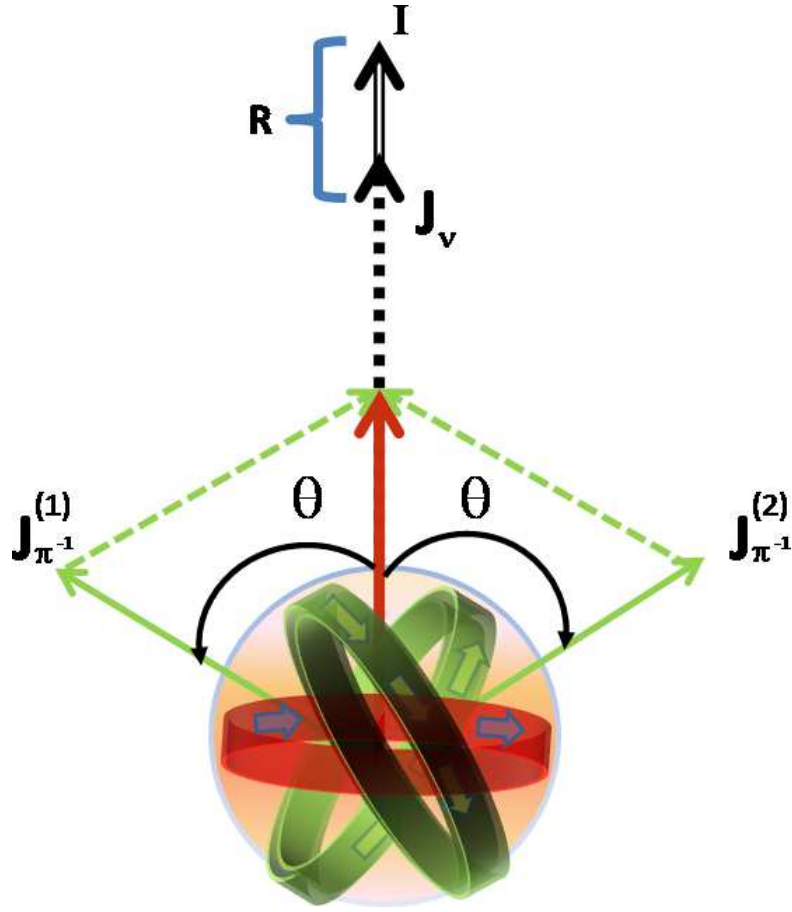


FIG. 1. The angular momentum vector diagram for AMR+rotation scenario where  $\mathbf{I}$ ,  $\mathbf{R}$ ,  $\mathbf{j}_{\pi}$  and  $\mathbf{j}_v$  are the total, rotational, proton hole and neutron particle angular momenta.

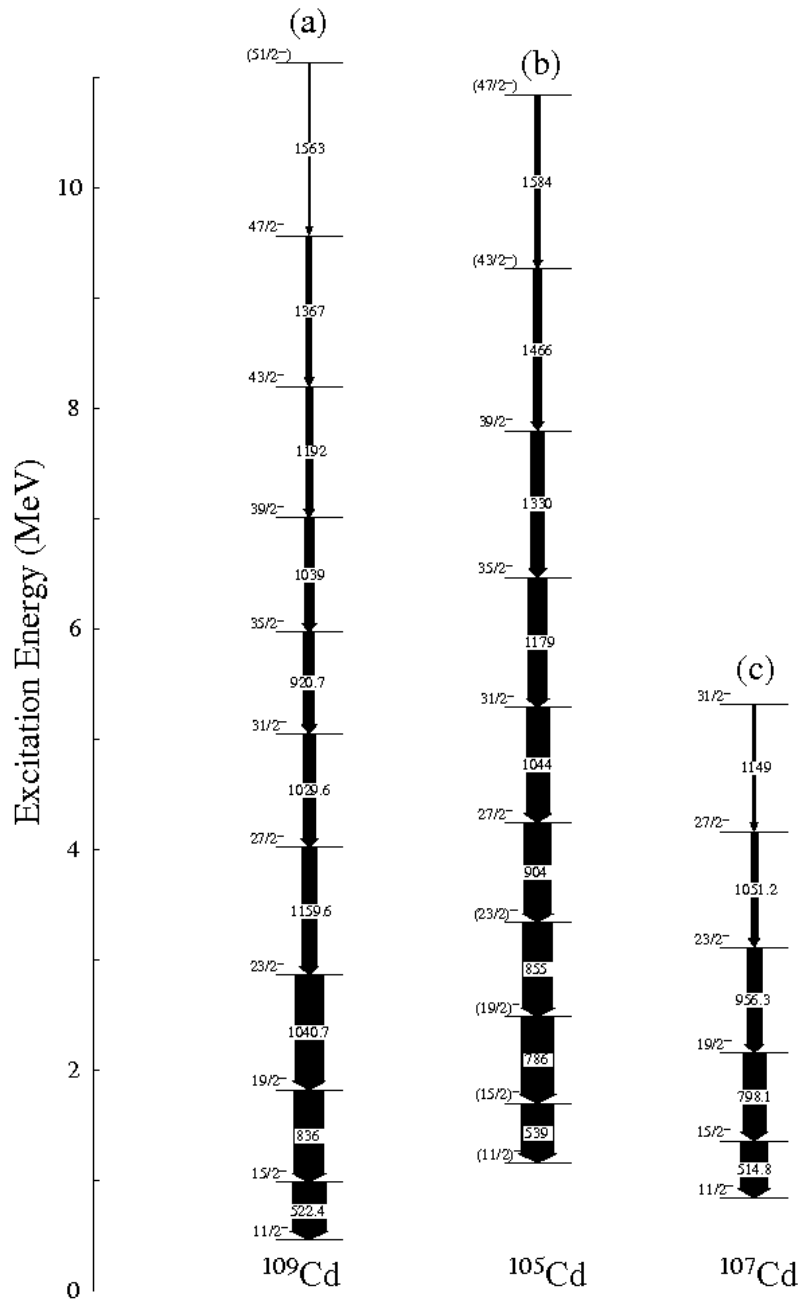


FIG. 2. Partial level schemes of the negative parity yrast bands of (a)  $^{109}\text{Cd}$  [10], (b)  $^{105}\text{Cd}$  [11] and (c)  $^{107}\text{Cd}$  [12].

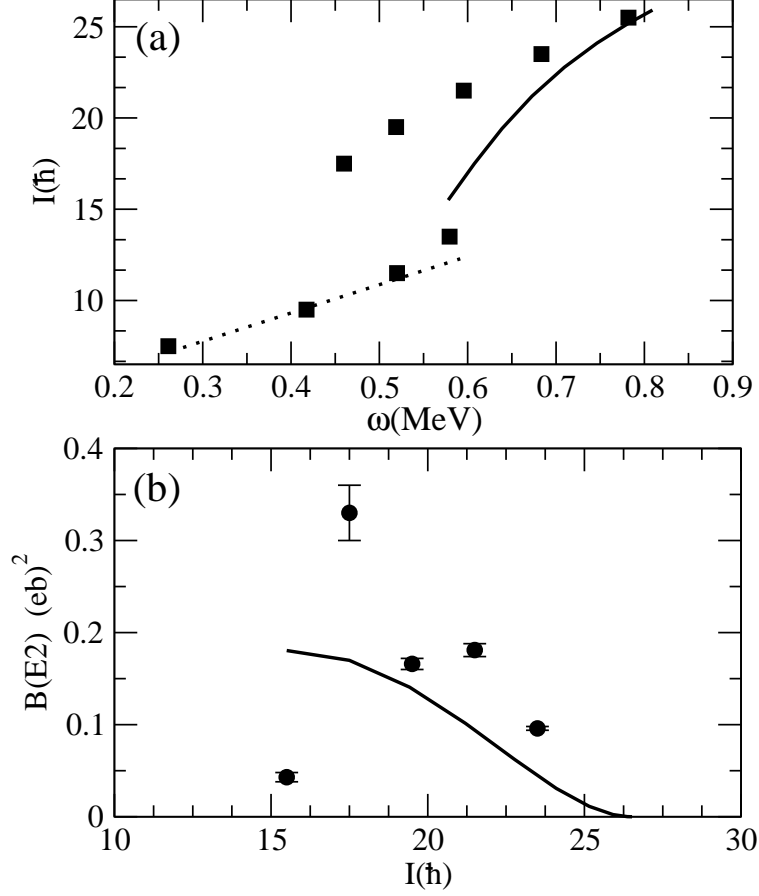


FIG. 3. The observed  $I(\omega)$  plots (a) and  $B(E2)$  values (b) in  $^{109}\text{Cd}$ . The solid line represents the calculated values using the classical particle rotor model for  $V_{\pi\nu} = 1.2 \text{ MeV}$ ,  $V_{\pi\pi} = 0.2 \text{ MeV}$ ,  $\mathfrak{S} \sim 6 \text{ MeV}^{-1} \hbar^2$  and  $\mathfrak{S}_{rot} \sim 15 \text{ MeV}^{-1} \hbar^2$ . The dashed line in (a) represents the  $I(\omega)$  plot for a rotor with moment of inertia  $15 \text{ MeV}^{-1} \hbar^2$  shifted by  $\sim 4\hbar$  along the y-axis.

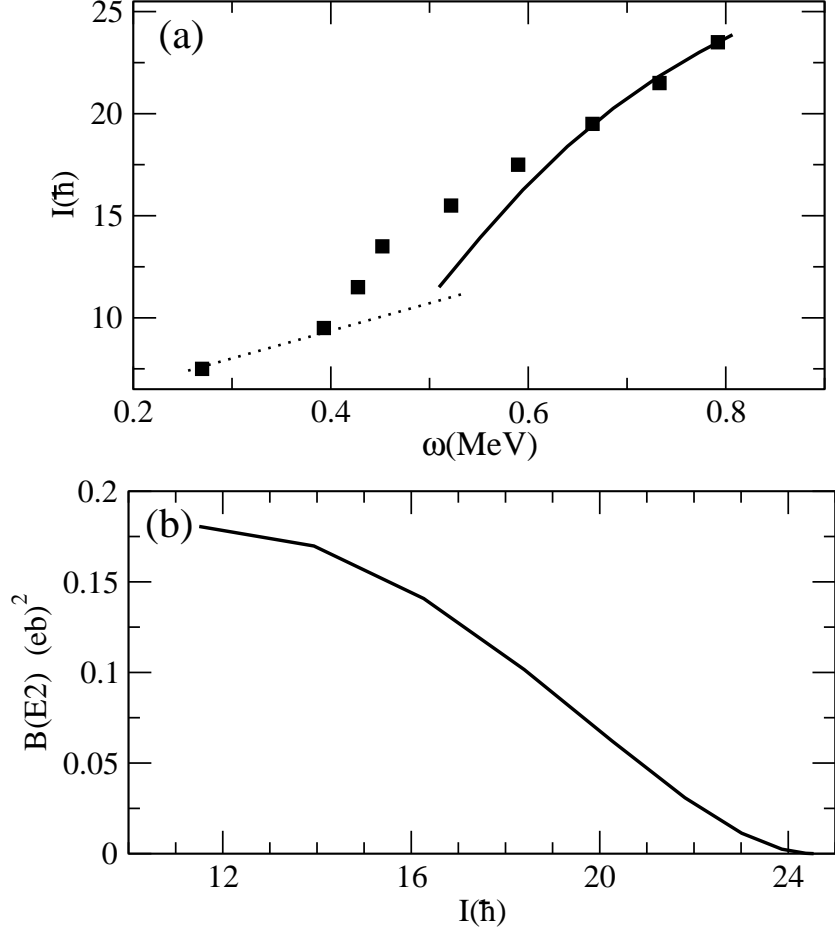


FIG. 4. The observed  $I(\omega)$  plots (a) and  $B(E2)$  values (b) in  $^{105}\text{Cd}$ . The solid line represents the calculated values using the classical particle rotor model for  $V_{\pi\nu} = 1.2 \text{ MeV}$ ,  $V_{\pi\pi} = 0.2 \text{ MeV}$ ,  $\mathfrak{S} \sim 11 \text{ MeV}^{-1} \hbar^2$  and  $\mathfrak{S}_{rot} \sim 15 \text{ MeV}^{-1} \hbar^2$ . The dashed line in (a) represents the  $I(\omega)$  plot for a rotor with moment of inertia  $15 \text{ MeV}^{-1} \hbar^2$  shifted by  $\sim 4\hbar$  along the y-axis.

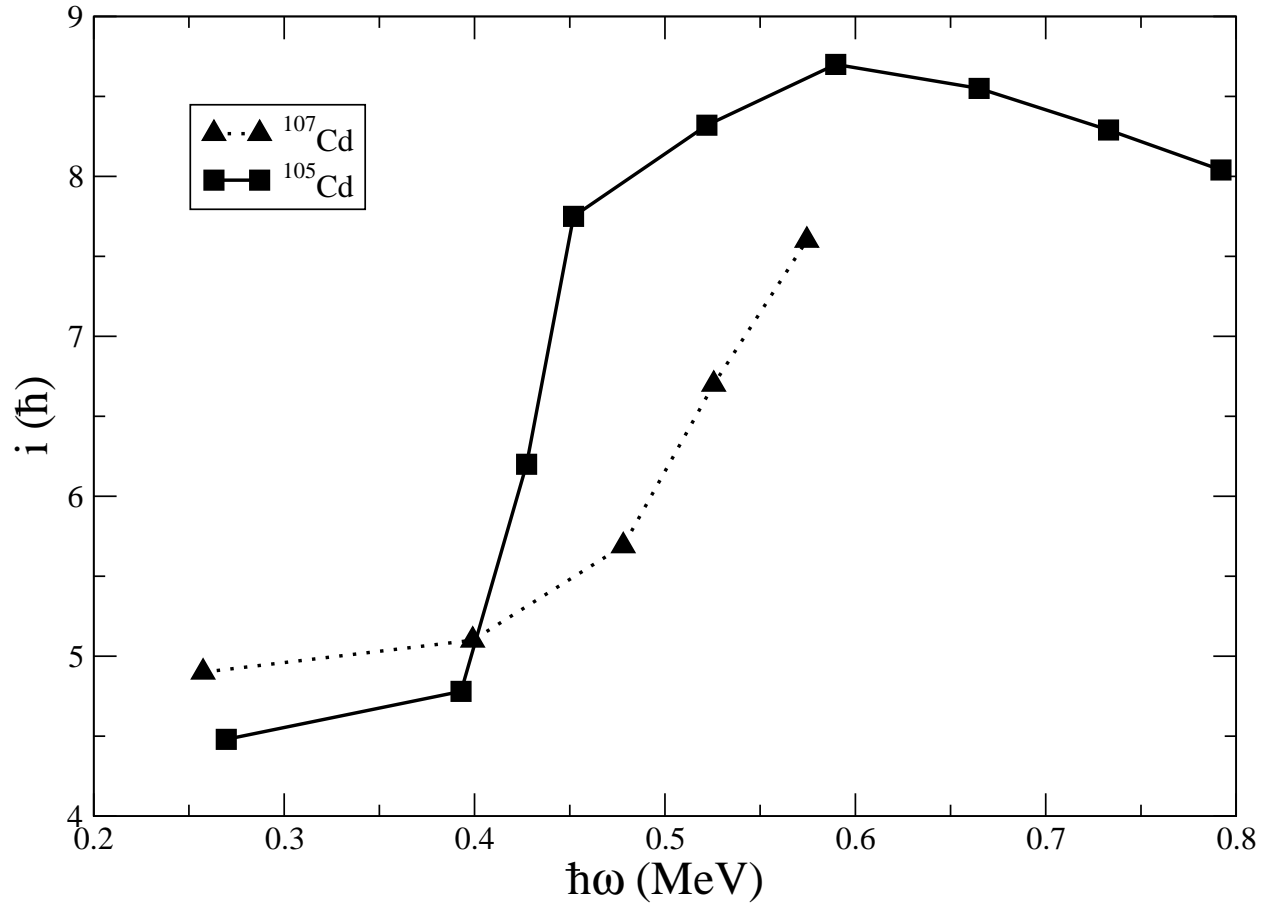


FIG. 5. Experimental aligned angular momentum for negative parity yrast band in  $^{105}\text{Cd}$  [11] (solid line) and  $^{107}\text{Cd}$  [12] (dotted line).

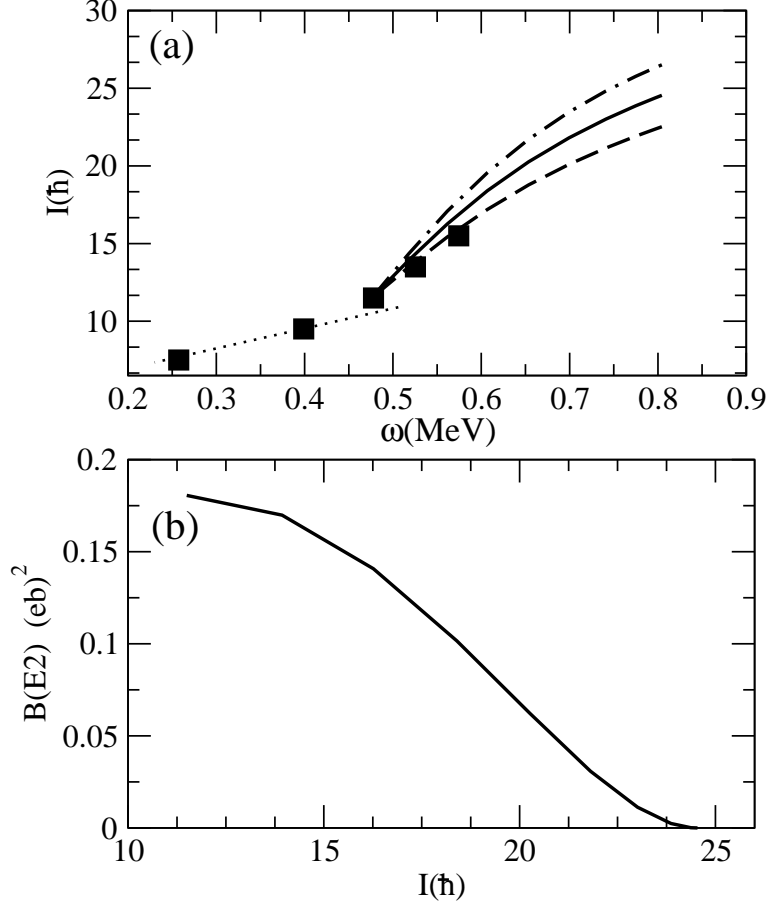


FIG. 6. The observed  $I(\omega)$  plots (a) and  $B(E2)$  values (b) in  $^{107}\text{Cd}$ . The dashed, solid and dot-dashed lines represents the calculated values for  $\mathfrak{S} \sim 6 \text{ MeV}^{-1} \hbar^2$ ,  $\mathfrak{S} \sim 11 \text{ MeV}^{-1} \hbar^2$  and  $\mathfrak{S} \sim 17 \text{ MeV}^{-1} \hbar^2$ , respectively. The other fixed parameters are  $V_{\pi\nu} = 1.2 \text{ MeV}$ ,  $V_{\pi\pi} = 0.2 \text{ MeV}$  and  $\mathfrak{S}_o = 14 \text{ MeV}^{-1} \hbar^2$ . The dotted line in (a) represents the  $I(\omega)$  plot for a rotor with moment of inertia  $15 \text{ MeV}^{-1} \hbar^2$  shifted by  $\sim 4\hbar$  along the y-axis.